Pergamon

Int. Comm. Heat Mass Transfer, Vol. 27, No. 6, pp. 775–783, 2000

0735-1933/00/$–see front matter

PII: S0735-1933(00)00158-5

THE EFFECT OF INERTIA ON VERTICAL FREE CONVECTION BOUNDARY LAYER FLOW FROM A HEATED SURFACE IN POROUS MEDIA WITH SUCTION

Nurzahan Banu and D. A. S. Rees
Department of Mechanical Engineering,
University of Bath, Claverton Down,
Bath, BA2 7AY, U.K.

(Communicated by J.P. Hartnett and W.J. Minkowycz)

ABSTRACT

A boundary layer analysis is performed for convection from a uniform temperature vertical heated surface in the presence of inertia and surface suction. The resulting boundary layer flow is non–similar and detailed solutions are presented. At relatively small distances from the leading edge surface suction is negligible and at large distances from the leading edge suction effects dominate for there the boundary layer attains a constant thickness. At any fixed value of x the boundary layer becomes thinner and the local rate of heat transfer increases as the rate of suction increases. The approach to the constant thickness state becomes more rapid as γ, the scaled rate of suction, increases. A detailed asymptotic analysis is undertaken which determine how quickly this asymptotic state is attained for large values of γ.

Introduction

This study deals with boundary layer flow induced by a heated semi–infinite surface embedded in a porous medium. Such configurations are of interest in modelling convetion from hot magma intrusions in subterranean aquifers; it was this aspect which motivated Cheng and Minkowycz [1] who considered a vertical heated surface. Corresponding horizontal plane and vertical axisymmetric configurations were analysed by Cheng and Chang [2] and Minkowycz and Cheng [3], respectively.

Most of the studies of flow in porous media assume that Darcy's law is valid. However this law is known to be valid only for relatively slow flows through the porous matrix. In general, we must consider the effect of fluid inertia, as well as of viscous diffusion at boundaries which may well become significant for materials with very high porosities, such as fibrous media and foams. Plumb and Huenefeld [4] treated the vertical configuration showing that the flow remains self–similar with the inclusion of inertia, but that the rate of heat transfer decreases as the inertia parameter increases, reflecting the increasing thickness of the boundary layer.

Merkin [5] considered the effect of uniform surface transpiration on Darcy convection from a vertical surface. A series expansion in powers of the square root of the distance from the leading edge was first obtained. This expansion was extended by a numerical solution of the full non-similar boundary layer equations. In the case of surface suction the boundary layer is found to approach a constant thickness and that the approach is through terms which are exponentially small for large x. Merkin [5] also considered the effect of surface blowing.

In this paper we extend Merkin's analysis by studying the combined effects of fluid inertia and surface suction on the boundary layer flow induced by a uniform temperature vertical surface embedded in a porous medium. At large distances from the leading edge suction effects dominate and boundary layer attains a constant thickness. Close to the leading edge suction is weak compared with buoyancy–induced convection and the flow field is but a perturbation of the Cheng and Minkowycz [1] flow. These behaviours are confirmed by a numerical solution using the Keller–box mthod. It is also found that the constant thickness solution is attained more quickly (in terms of x) as the suction rate increases — an asymptotic analysis for larger rates of suction quantifies this speed of attainment.

Governing Equations

We consider a heated vertical surface which is embedded in a homogenous fluid–saturated porous medium through which fluid is withdrawn at a uniform rate. The surface is held at the constant temperature, T_1 whilst the ambient temperature of the medium is T_0. We assume that $T_1 > T_0$ and examine the two dimensional flow which is induced by buoyancy forces along the surface. We take as our governing equations,

$$\frac{\partial u'}{\partial x'} + \frac{\partial v'}{\partial y'} = 0, \tag{1}$$

$$\frac{K}{\mu}\Big[-\frac{\partial p}{\partial x'} + \rho g \beta (T - T_0)\Big] = \Big[1 + \frac{\tilde{K}}{\mu}\rho q'\Big]u' \qquad \frac{K}{\mu}\Big[-\frac{\partial p}{\partial y'}\Big] = \Big[1 + \frac{\tilde{K}}{\mu}\rho q'\Big]v' \tag{2,3}$$

$$u'\frac{\partial T}{\partial x'} + v'\frac{\partial T}{\partial y'} = \kappa\Big[\frac{\partial^2 T}{\partial x'^2} + \frac{\partial^2 T}{\partial y'^2}\Big] \tag{4}$$

where primes indicate dimensional variables. In equations (1-4) x' and y' are the Cartesian coordinates along and perpendicular to the heated plate, respectively, u' and v' are the respective fluid velocity fluxes, β is the coefficient of cubical expansion, and κ the thermal diffusivity of the staurated medium. Further, q' is the fluid flux speed which is given by $(q')^2 = (u')^2 + (v')^2$. In (2) and (3) K is the permeability of the medium and $\tilde{K}$ is a material parameter which may be thought of as a measure of the inertial inpedance of the matrix. ρ is the fluid density, μ the coefficient of viscosity, p is the dynamic pressure, and g is the acceleration due to gravity.

Equations (1)-(4) may be nondimensionalized by introducing the substitutions

$$(x', y') = l(x, y), \qquad (u', v') = \frac{\kappa}{l}(u, v), \qquad T = T_0 + (T_1 - T_0)\theta, \tag{5c}$$

where l is a macroscopic lengthscale, and by defining a stream function ψ, such that

$$(u, v) = (\frac{\partial\psi}{\partial y}, -\frac{\partial\psi}{\partial x}) + (0, -Ra^{1/2}). \tag{6}$$

The second term on the right hand side of (6) accounts for the uniform suction velocity into the vertical surface. The size of this term is such that the present analysis fits into the theroretical framework of Cheng and Minkowycz [1]. On elimination of the pressure terms theres result the following equations,

$$\left(1 + \frac{\gamma Q}{Ra}\right)\nabla^2\psi + \left(\frac{\gamma}{QRa}\right)(\psi_x^2\psi_{xx} + 2\psi_x\psi_y\psi_{xy} + \psi_y^2\psi_{yy}) = Ra\ \theta_y, \tag{7}$$

$$\nabla^2\theta + \theta_y Ra^{-1/2} = \psi_y\theta_x - \psi_x\theta_y. \tag{8}$$

The Darcy-Rayleigh number Ra and the Darcy-Grashof number, γ, are given by

$$Ra = \frac{\rho g\beta K(T_1 - T_0)l}{\mu k}, \qquad \gamma = \left(\frac{\rho}{\mu}\right)^2 K\tilde{K}g\beta(T_1 - T_0). \tag{9,10}$$

The term Q is a dimensionless fluid flux given by $Q^2 = \psi_x^2 + \psi_y^2$, and ∇^2 is the two-dimensional Laplacian. The terms involving $Ra^{-1/2}$ in (6) and (8) arise from assuming that the dimensional suction velocity is precisely $\frac{\kappa}{l}Ra^{-1/2}$; not only is this magnitude sufficiently large that it affects the boundary layer flow when $x = O(1)$, but this velocity scale allows the definition of a natural length scale for the flow, as follows. If V denotes the magnitude of the suction velocity, then $V = \frac{\kappa}{l}Ra^{-1/2}$ may be rearranged to yield

$$l^3 = \frac{\kappa^2 K\mu}{g\beta(T_1 - T_0)V^2} \tag{11}$$

where all the terms on the right hand side are known for a particular configuration.

Boundary Layer Analysis

If we assume that $x = O(1)$ as $Ra \to \infty$, then the boundary layer approximation is valid when $y \ll 1$. Under these conditions, equations (7) and (8) reduce to

$$\Big(1 + 2|\psi_y|\gamma Ra^{-1}\Big)\psi_{yy} = Ra\theta_y, \qquad \theta_{yy} + \theta_y Ra^{-1/2} = \psi_y\theta_x - \psi_x\theta_y \tag{12,13}$$

and are subject to the boundary conditions,

$$\psi = 0, \;\; \theta = 1 \quad \text{on} \quad y = 0, \tag{14}$$

$$\frac{\partial\psi}{\partial y} \to 0, \; \theta \to 0 \quad \text{as} \quad y \to \infty. \tag{15}$$

We now introduce the following boundary layer scalings

$$\psi = Ra^{1/2}\hat{\psi}, \quad y = Ra^{-1/2}\hat{y}, \quad x = \hat{x}, \quad \theta = \hat{\theta}, \tag{16}$$

into equations (12) and (13). We obtain the following equations:

$$\Big(1 + \gamma\hat{\psi}_{\hat{y}}\Big)\hat{\psi}_{\hat{y}\hat{y}} = \hat{\theta}_{\hat{y}}, \qquad \hat{\theta}_{\hat{y}\hat{y}} + \hat{\theta}_{\hat{y}} = \hat{\psi}_{\hat{y}}\hat{\theta}_{\hat{x}} - \hat{\psi}_{\hat{x}}\hat{\theta}_{\hat{y}}. \tag{17,18}$$

In (17) we have omitted the moduli around $\hat{\psi}_{\hat{y}}$ since this quantity is always positive. Now we have to introduce a set of pseudo-similarity variables, (ξ, η), the η value of which, in the absence of inertia and suction effects, corresponds precisely to the similarity variable used in Cheng and Minkowycz [1]:

$$\hat{\psi} = \hat{x}^{1/2} f(\eta, \xi), \qquad \hat{\theta} = g(\eta, \xi), \qquad \eta = \frac{\hat{y}}{\hat{x}^{1/2}}, \qquad \xi = \hat{x}^{1/2} \tag{19}$$

Equations (17) and (18) reduce to the forms

$$(1 + \gamma f')f'' = g', \qquad g'' + \xi g' + \tfrac{1}{2} f g' = \tfrac{1}{2}\xi(f' g_\xi - f_\xi g') \tag{20,21}$$

The corresponding boundary conditions are

$$\eta = 0: \; f = 0, \; g = 1 \qquad \text{and} \qquad \eta \to \infty: \; f' \to 0, \; g \to 0. \tag{22}$$

If we integrate equation (20), rearrange the resulting expression and set $\eta = 0$, then we get the following expression for the slip velocity:

$$f'(0) = \frac{2}{1 + \sqrt{1 + 2\gamma}}. \tag{23}$$

From this simple analysis we see that the slip velocity decreases as γ increases which reflects the increasing resistance to flow. When γ is very large we have the asymptotic relation $f'(0) \sim (2/\gamma)^{1/2}$.

Numerical Results

A complete numerical solution uses the Keller–Box scheme to integrate the sets of equations (20,21) for $\hat{x} \ll 1$ and (17,18) for $\hat{x} \gg 1$; these separate sets of equations are used in their appropriate domains of validity. The latter equations are taken because the final asymptotic state is a boundary layer of uniform thickness where $\hat{y}$ may be taken as the similarity variable. Integration proceeds in a stepwise manner from $\hat{x} = 0$. The equations are first reduced to first order form in η or $\hat{y}$, and are discretised using central differences based halfway between the grid points in both directions. Such a central difference scheme gives second order accuracy. There results a set of nonlinear difference equations for the unknown variables at $\hat{x} = \hat{x}_i$ in terms of their values at $\hat{x} = \hat{x}_{i-1}$. The difference equations are solved iteratively using the multi-dimensional Newton–Raphson method where the Jacobian matrix is computed numerically. For a given value of ξ or $\hat{x}$, the iterative procedure is stopped when the maximum absolute pointwise change between successive iterates is less than 10^{-8}. Given the very different similarity forms at the leading edge and far downstream, it is necessary to present the evolution with $\hat{x}$ of the surface rate of heat transfer in two forms, each being appropriate for its own regime. Therefore one a set of curves presented in Fig. 1 is suitable for describing well the heat transfer near the leading edge and is given by

$$-\hat{\theta}_\eta \quad \text{for} \quad \hat{x} \ll 1 \qquad \text{and} \qquad -\hat{x}^{1/2}\hat{\theta}_{\hat{y}} \quad \text{for} \quad \hat{x} \gg 1, \tag{24}$$

and the other set, presented in Fig. 2, is more appropriate for viewing the approach to the suction–dominated state and is given by

$$-\hat{x}^{1/2}\hat{\theta}_\eta \quad \text{for} \quad \hat{x} \ll 1 \qquad \text{and} \qquad -\hat{\theta}_{\hat{y}} \quad \text{for} \quad \hat{x} \gg 1, \tag{25}$$

Both graphs are plotted against $\xi = \hat{x}^{1/2}$ for different values for γ.

Near the leading edge suction effects are weak and the rate of heat transfer corresponds exactly to those given in [6]. The decreasing rate of heat transfer as γ grows is a direct consequence of the decreasing ability of buoyancy forces to drive the flow. Therefore heat conducts more easily from the heated surface and the boundary layer thickens. At increasing distances from the leading edge suction effects become more important. This causes the boundary layer to become thin relative to when suction is absent, and hence the rate of heat transfer, as given by (24), increases with $\hat{x}$. At large distances, (25) is the more appropriate formula to use to present the rate of heat transfer. From Figure 2 we see that the approach to the constant–thickness state becomes more rapid as γ increases, a qualitative confirmation of the analysis of the next subsection. Again, the decreasing streamwise velocity caused by increasing inertia effects renders suction more effective and explains why the approach to the asymptotic state becomes more rapid as γ increases.

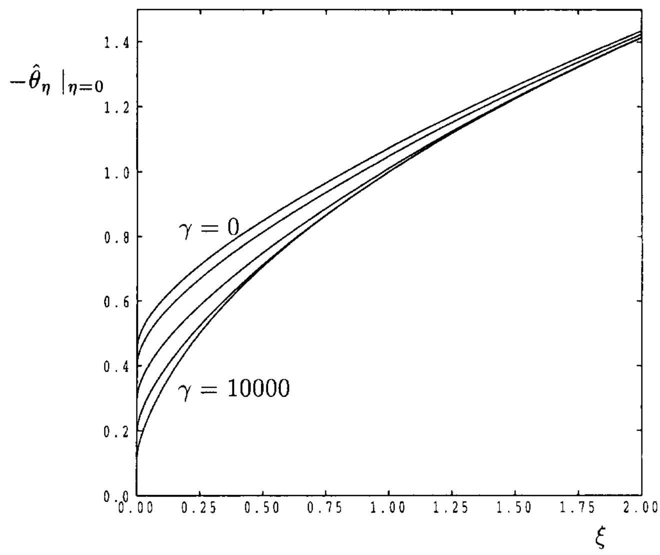

FIG. 1.
The rate of heat transfer given by $-\hat{\theta}_\eta \mid_{\eta=0}$ for $\gamma = 0, 1, 10, 100, 10000$.

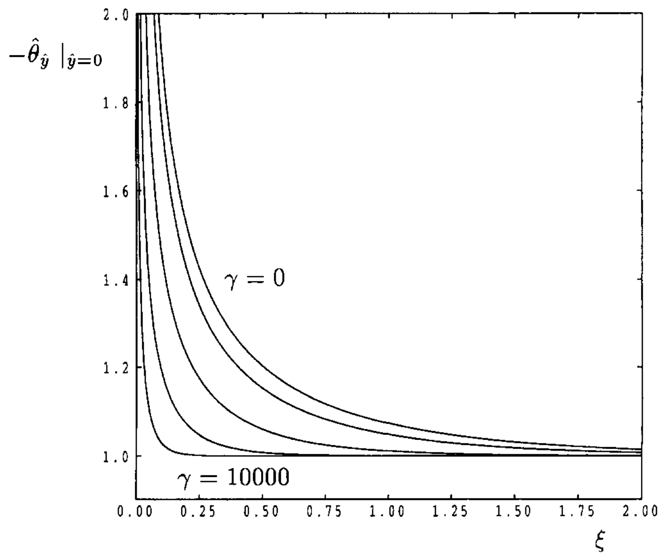

FIG. 2.
The rate of heat transfer given by $-\hat{\theta}_{\hat{y}} \mid_{\hat{y}=0}$ for $\gamma = 0, 1, 10, 100, 10000$.

Asymptotic Analysis

Given the results of Merkin [5] on the effects of suction without inertia, it was to be expected that the boundary layer should attain a constant thickness for large values of $\hat{x}$. Equations (17) and (18) admit the straightforward $\hat{x}$–independent solutions,

$$\hat{\theta} = e^{-\hat{y}} \equiv \hat{\theta}_B \qquad \hat{\psi} = \frac{2e^{-\hat{y}}}{1+\sqrt{1+2\gamma e^{-\hat{y}}}} \equiv \hat{\psi}_B, \tag{26}$$

where the B–subscript denotes the basic solution. The detailed approach to this solution is found by perturbing equations (17) and (18) about the solution given in (26). Therefore we substitute

$$\hat{\psi} = \hat{\psi}_B + F(\hat{y})e^{\lambda\hat{x}}, \qquad \hat{\theta} = \hat{\theta}_B + G(\hat{y})e^{\lambda\hat{x}} \tag{27a, b}$$

into equations (17) and (18) and linearise to obtain the equations

$$(1+\gamma\hat{\psi}_B')F'' + \gamma F'\hat{\psi}_B'' = G', \qquad G'' + \alpha G' = \lambda(\hat{\psi}_B' G - F\hat{\theta}_B') \tag{28, 29}$$

Integrating equation (28) once, we get

$$F' = G/(1+\gamma\hat{\psi}_B') \tag{30}$$

Equations (29) and (30) were solved subject to $F(0) = G(0) = G(\infty) = 0$ and $G'(0) = 1$ to obtain values for λ, the exponential rate of growth of the perturbation. Solutions were obtained using a straightforward shooting method with the fourth order Runge-Kutta scheme. The four boundary conditions together with the 3^{rd} order system, (29) and (30), were supplemented by the fourth equation, $\lambda' = 0$. It is found that the value of λ varies over many orders of magnitude and therefore numerical values are given in Table 1.

TABLE 1

Values of λ for various values of γ.

γ	λ	$\lambda/\sqrt{\gamma}$
0	−1.4458	∞
1	−1.7579	−1.7579
2	−1.9814	−1.4011
5	−2.4691	−1.1042
10	−3.0461	−.9633
20	−3.8804	−.8677
50	−5.5540	−.7855
100	−7.4494	−.7449
10000	−65.8408	−.6584
1000000	−649.8129	−.6498
100000000	−6489.5311	−.6490

When $\gamma = 0$ we recover the result of Merkin [5], that $\lambda = -1.4458$. It is clear from Table 1 that the rate of decay increases rapidly as inertia effects become stronger. Furthermore λ seems to become proportional to $\gamma^{1/2}$ at leading order when γ is very large; this observation motivates the following asymptotic analysis.

We take $\gamma \gg 1$, and we assume that $y \ll (ln\gamma)^{-1}$, (i.e. that $\gamma e^{-y} \gg 1$; see (26)) and therefore we may take $1 + 2\gamma e^{-y} \sim 2\gamma e^{-y}$. Hence we have

$$\hat{\psi}'_B \sim \sqrt{\frac{2}{\gamma}} e^{-y/2}, \tag{31}$$

and therefore the momentum equation (30) and the energy equation (29) reduce to

$$F' \simeq \frac{Ge^{y/2}}{\sqrt{2\gamma}} \qquad G'' + G' = \lambda \Big[\sqrt{\frac{2}{\gamma}} e^{-y/2} G + e^{-y} F \Big]. \tag{32, 33}$$

Given the results shown in the third column of Table 1 we rescale according to

$$\lambda = \bar{\lambda}\sqrt{\gamma}, \qquad G = \bar{G} \qquad \text{and} \qquad F = \frac{\bar{F}}{\sqrt{\gamma}}. \tag{34}$$

and let $\gamma \to \infty$. Equations (32) and (33) reduce to the following form at leading order,

$$\bar{F}' = \frac{1}{\sqrt{2}} e^{y/2} \bar{G}, \qquad \bar{G}'' + \bar{G}' = \bar{\lambda} \Big[\sqrt{2} e^{-y/2} \bar{G} + e^{-y} \bar{F} \Big] \tag{35, 36}$$

and these are to be solved subject to the boundary conditions,

$$\bar{F}(0) = 0, \quad \bar{G}(0) = 0, \quad G'(0) = 1 \quad \text{for} \quad y = 0 \qquad \text{and} \qquad G \to 0 \quad \text{as} \quad y \to \infty \tag{37}$$

We find that $\bar{\lambda} = -0.6490$, which confirms to 4 decimal places the asymptotic behaviour of λ indicated by the third column of Table 1. Figure 3 shows how $\log_{10}(-\lambda)$ varies with $\log_{10}(\gamma)$; when $\gamma \geq 10^6$ the asymptotic results are correct to at least three figures.

Conclusion

We have extended Merkin's [5] analysis of the effect of suction on free convective boundary layer flow from a vertical surface in a porous medium by introducing Forchheimer inertial effects. In the absence of suction these terms cause the boundary layer to become thicker, and the surface of heat transfer to decrease, but the solutions remain self-similar. (see [4] and [5]). However, suction causes the boundary layer equations to be nonsimilar.

Near the leading edge suction effects are weak and the rate of heat transfer corresponds exactly to those given in [6] The decreasing of the rate of heat transfer as the inertia effect strengthens is a direct consequence of the decreasing ability of the buoyancy forces to

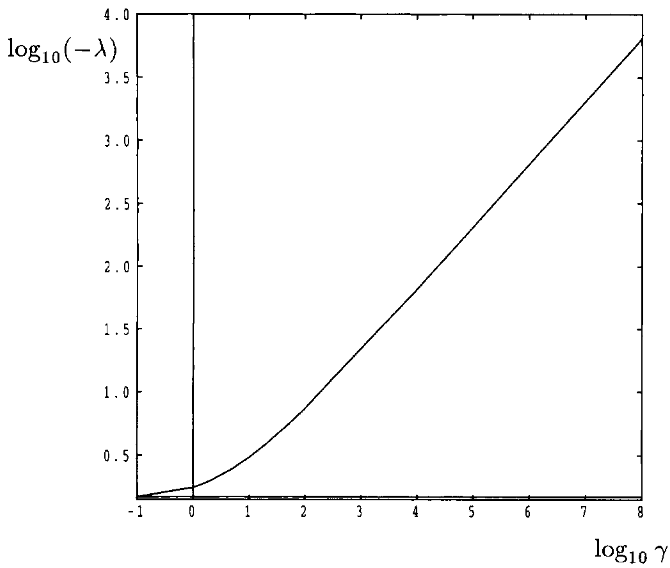

FIG. 3.
The variation of the rate of decay with γ.

drive the flow. Far from the leading edge suction effects dominate, and the boundary layer attains a constant-thickness state. This approach is more rapid as γ increases. Table 1 gives the rate of decay towards the uniform state, and we see that this increases rapidly as γ increases and we see that λ becomes proportional to $\sqrt{\gamma}$ at leading order when γ is very large. An asymptotic analysis has confirmed this numerical result.

Acknowledgement

The first-named author would like to thank the University of Bath for a Research Studentship to enable this research to be undertaken.

References

1. P. Cheng and W.J. Minkowycz, *J. Geophys. Res.* **82**, 2040-2044, (1977).
2. P. Cheng and I.D. Chang, *Int. J. Heat Mass Transfer* **19**, 1267-1272, (1976).
3. W.J. Minkowycz, and P. Cheng, *Int. J. Heat Mass Transfer* **19**, 805-813, (1976).
4. O.A. Plumb, and J.C. Huenefeld, *Int. J. Heat Mass Transfer* **24**, 765-768, (1981).
5. J.H. Merkin, *Int. J. Heat Mass Transfer* **21**, 1499-1504, (1978).
6. D.S. Riley, and D.A.S. Rees, *Q. J. Mech. Appl. Math.* **38**, 277-295, (1985).

Received June 30, 2000